

Chapter 8

Paper submitted as a contribution in the symposium "*Dental Perspectives on Human Evolution: State of the Art Research in Dental Palaeoanthropology*" held at the Max Planck Institute in Leipzig, Germany, May 2005.

PORTABLE CONFOCAL SCANNING OPTICAL MICROSCOPY OF AUSTRALOPITHECUS AFRICANUS ENAMEL MICROSTRUCTURE

Timothy G. BROMAGE

*Hard Tissue Research Unit
Dep'ts of Biomaterials & Basic Sciences
New York University College of Dentistry
345 East 24th Street
New York, NY 10010-4086
USA
Email: tim.bromage@nyu.edu*

Rodrigo S.LACRUZ

*Institute for Human Evolution
B.P.I. for Palaeontological Research
University of the Witwatersrand
P. Bag 3 WITS 2050
Johannesburg
South Africa
Email: LacruzR@science.pg.wits.ac.za*

Alejandro PEREZ-OCHOA

*Department of Paleontology
Universidad Complutense de Madrid
Madrid 28040
Spain
Email: perezochoa@msn.com*

Alan BOYDE

*Hard Tissue Research Unit
Dental Biophysics
Queen Mary University of London
New Road
London E1 1BB
England
Email: a.boyde@qmul.ac.uk*

ABSTRACT

The study of hominid enamel microstructural features is usually restricted to the examination of fortuitous enamel fractures by low magnification stereo-zoom microscopy or, rarely, because of its intrusive nature, by high magnification compound microscopy of ground thin sections. To contend with limitations of magnification and specimen preparation, a Portable Confocal Scanning Optical Microscope (PCSOM) has been specifically developed for the non-contact and non-destructive imaging of early hominid hard tissue microstructure. This unique instrument can be used for high resolution imaging of both the external features of enamel, such as perikymata and microwear, as well as internal structures, such as cross striations and, commonly, the cuspal striae, from naturally fractured or worn enamel surfaces. Because there is veritably no specimen size or shape that cannot be imaged (e.g. fractured enamel surfaces on intact cranial remains), study samples may also be increased over what would have been possible before. We have applied this innovative technology to the study of enamel microstructural features from naturally occurring occluso-cervical fractures of the South African hominid, *Australopithecus africanus* representing different tooth types. We present for the first time detailed information regarding cross striation periodicity for this species and, in addition, we present data on striae-EDJ angles in a large sample of teeth and crown formation time for a molar of *A. africanus*. Our results characterize a pattern of enamel development for *A. africanus*, which is different to that reported for the genus *Paranthropus*, as previously observed.

Keywords: portable confocal microscope, hominid skeletal microstructure

Running Head: Confocal Microscopy of *A. africanus* Enamel

Introduction

Most fossils are either translucent or, if they are surface reflective, are not flat. In both cases, light interacts with the sample over a considerable vertical range and is reflected (or the fluorescent light emanates) from a thick layer. We have found a solution to this imaging challenge in development of portable confocal microscopy for the evaluation of rare and unique early hominid fossils.

The principle of the Portable Confocal Scanning Optical Microscope (PCSOM) is to eliminate the scattered, reflected, or fluorescent light from out of focus planes, allowing only light originating from the plane of focus of the objective lens to contribute to image formation. It does this at the several conjugate focal planes (intermediate, eye point, image recording device), and thus eliminates light coming from all out of focus planes. In practice, an illuminated spot in the plane of focus is scanned across the field of view and an image is compiled. Confocal scanning optical microscopy thus differs from conventional light microscopy, where light from the focus plane of the objective lens, as well as from all out of focus planes across the entire field of view, is observed. The history and various technical achievements in confocal microscopy are summarized in Boyde (1995).

Beyond a simple description of the PCSOM, we report here initial studies using this technology to assess *Australopithecus africanus* crown formation time, cross striation periodicity, and variation on the enamel extension rate for selected teeth. *A. africanus* derives from the Tufa deposits at Taung and the limestone caves of Sterkfontein and Makapansgat. The temporal range of this species is still a matter of debate (e.g. Berger *et al.*; 2002), but based upon faunal evidence a Late Pliocene age, roughly from 2.9-2.4 m.y., is indicated (Delson, 1984, 1988; Vrba, 1995). The phylogenetic placing of *A. africanus* and its relationship with other broadly contemporaneous hominids is also unresolved (Berger *et al.*; 2002; Tobias, 1980; White *et al.*; 1981). In this regard, enamel developmental parameters may be particularly useful in interpreting such relationships, providing strong bases for comparisons between species (Grine and Martin, 1988).

Materials and Methods

THE MICROSCOPE

We employ a PCSOM based on the Nipkow disk technique (Nipkow, 1884) described in detail by Petran and Hadravsky (e.g., 1966) and first commercialized in the early 1980's. The Petran and Hadravsky design uses a so-called two sided disc; the specimen is

illuminated through an array of pinholes on one side of the disc whilst detected through a conjugate array of pinholes on the other (via a number of delicately aligned mirrors). Applications of this technology to bone and tooth microstructure were demonstrated by Boyde et al. (1983). Another Nipkow disk design employs a single-sided disk in which the illumination and detection pinhole is one in the same (Kino, 1995). This latter design sacrifices slightly better quantum efficiency for a robust construction that is able to tolerate our relatively extreme portable applications.

To date we have developed two versions of the PCSOM; the 1K2 (Figure 1) and the 2K2 (Figure 2). Both employ a one-sided Nipkow disc Technical Instrument Co. K2S-BIO confocal module (Zygo Corp., Sunnyvale, CA), specifically configured to deal with the challenging imaging problems encountered in paleoanthropology (Bromage, 2003). Like other confocal scanning optical microscopes, the final image derives from the focused on plane. Thus, it eliminates the fog due to the halo of reflected, scattered or fluorescent light above and below the plane of focus, which otherwise confounds image content in conventional light microscopy.

An interesting feature of the single-sided disk design by Kino (1995) is the approach taken to suppress internal, non-image-related reflections that are otherwise a significant problem in this type of system; the classical method of illuminating with polarized light to stop light reflections from within the optical system (e.g. from optical hardware within the body of the microscope), but not the useful light reflecting from the specimen and returning through the objective lens. Linear polarizing light filters and a single quarter-wave plate are employed for this purpose. This design significantly reduces the number of mirrors in the light path making the alignment of the optics less critical. The result is a very robustly constructed instrument able to tolerate transport and relatively rough handling (e.g., as checked-in baggage for air travel).

The microscope configurations include several other features critical to our research. Consideration was given to obtaining objective lenses with relatively long working distances (i.e., ca. 20 mm) for both the 1K2 and the 2K2. Often we have little control over the geometry of broken fossil bone surfaces examined under remote field or museum conditions, and so we must be prepared to image through long Z-height positions to avoid mechanical interference between the bone and the objective nosepiece. Objectives chosen include 5x and 10x lenses (34 mm and 19 mm working distances respectively; Thales-Optem Inc., Fairport, NY, USA) and Mitutoyo 20x and 50x lenses (20 mm and 13 mm working distances respectively; Mitutoyo Asia Pacific Pte Ltd,

Singapore). Flexibility in magnification is achieved by both the introduction of a Thales-Optem 0.5x or 1.9x CCD adapter or by converting the fixed magnification optical assembly described above into a zoom system, which involves the introduction of a Thales-Optem 70XL zoom module (1-7x) between the K2S-BIO module coupler and the manual coarse/fine focus module. For fully automated image acquisition, we motorized the Z focus (below).

Automation in X, Y, and Z axes has been variously implemented onto the PCSOM. The 1K2 includes a motorized RS232 Z-stepping motor control setup (Thales-Optem Inc., Fairport, NY, USA) in place of the manual coarse/fine focus module when automation is desired. This setup includes an independently powered OEM board connected to a stepping motor fitted to a focus module and the serial port of the computer. Included software permits one to drive the focus to stored set positions between the desired ends of travel, or to incrementally drive the focus by any stipulated distance until all optical planes within the field of view have been imaged. Movement in X and Y axes is carried out on a manual microscope stage. The 2K2 includes a KP53 motorized precision micro-stepping X-Y stage from the Semprex Corporation (Campbell, CA, USA), and a Vexta 2-phase Z-axis stepping motor (Oriental Motor USA Corp., Torrance, CA, USA). Integrated XYZ movement is performed by an Oasis 4i PCI stepper motor controller board for XY stage and Z focus. A three-axis trackball/mouse control of XYZ axes allows manual stage and focus movement to aid real-time viewing.

Portable image acquisition are transmitted through the FireWire™ IEEE 1394 digital interface now common on notebook and desktop computers, thus eliminating the need for a framegrabber. The 1K2 uses a 4-pin IEEE 1394 high resolution 12 bit monochrome QIMAGING Retiga 1300 camera (Burnaby, BC, Canada), which has a 2/3" monochrome progressive scan interline CCD containing 1280 x 1024 pixels. Real-time image previewing capability facilitates camera setup conditions, which are adjusted by software interface. Adjustments include integration time, gain, and offset. The 2K2 uses a JVC KY-F1030U 6-pin IEEE 1394 digital camera containing a 1/2" color progressive scan interline CCD and 1360 x 1024 output pixels, operating at 7.5 frames per second live.

The 175W (1K2) and 300W (2K2) Lambda LS Xenon Arc Lamps (Sutter Instrument Company, Novato, CA, USA) transmit a flat and intense beam of light via a liquid light guide. It operates at wavelengths suitable for both fluorescence and white light illumination (320nm to 700nm output in an ozone-free bulb), is robustly constructed

and pre-aligned, and is economically packaged and lightweight, housing its own power supply.

The 1K2 employs A Sony VAIO Mobile Pentium notebook PC computer for image capture. We currently use a VAIO SRX27 (800MHz; 256k RAM; Windows XP). It weighs less than 3 pounds, thus satisfying our need for maximum portability, and it contains a 4-pin IEEE 1394 interface. A Shuttle XPC SB52G2 computer with a Pentium4 Intel processor and Windows XP Professional (Shuttle Computer Group Inc., Los Angeles, CA, USA) supports fully automated XYZ stage movement and image acquisition. A reasonably lightweight and thin standard 1024x768 15" monitor (Dell Inc., Round Rock, TX, USA) was chosen for our real-time viewing.

The microscope returns image detail from a very thin optical plane at and immediately below the object surface (1-50 micrometers, depending upon specimen characteristics). To obtain two- or three-dimensional projections from a surface which is anything but perfectly flat, potential fields of view must be compiled from a through-series of captured images at all optical planes represented in the Z-axis. Computerized control over image acquisition for both the 1K2 and 2K2 using Syncroscopy Auto Montage software (Syncroscopy Inc., Frederick, MD, USA) permits an even and fully representative image of either a pseudo-planar field of view or a three-dimensional reconstruction of surface or sub-surface details. Figure 3 is a completely in-focus surface reflection image of fractured and topographically complex *Paranthropus robustus* molar enamel, Application of a coverslip and clearing medium (see below) permits this field of view to be collapsed into a 2D image of its contained enamel microstructure (Figure 4). For extensive automated XY image montaging with the 2K2, Syncroscopy Montage.Explorer (Syncroscopy Inc., Frederick, MD, USA) software is employed, which can operate in "3D mode" to acquire useful Z focal planes over fields as large as 40,000 x 40,000 pixels.

The custom stands for both the 1K2 and 2K2 are simple and lightweight. The 1K2 stand consists of three 1/2 in thick Garolite sheet grade platforms supported by four 1 in diameter, 24 in length, ceramic coated hardened precision aluminum shafts. Each shaft is secured to bottom platform flange mounts. The K2S-BIO module rests on a neoprene pad on the central sliding platform, along which each shaft glides through a 1 in bore Frelon-lined fixed alignment anodized aluminum linear bearing. The top platform bolts to the ends of the shafts in order to stabilize the stand. The central sliding platform is secured at any desired vertical position by a 1 in bore aluminum clamp on each shaft

below the platform bearings. This platform has a forward aperture through which the K2S-BIO objective assembly passes. The bottom platform has an identical aperture through which the objective assembly can be lowered to image objects of any size permitted below the table top.

The 2K2 stand is composed of aluminium and includes an upright cylinder, containing within a lead screw operable from above, which drives the Nipkow disk module platform up or down; the drive is sensitive enough to be used as a coarse focus adjustment. The cylinder inserts into a sleeve at the base from which two hollow rectangular feet slide forward and rotate out at any angle appropriate for the balance of weight and required workspace. The platform for holding the K2S-BIO attaches to a sleeve around the cylinder, which rides on a bearing that conveys the module in any rotational position within the workspace.

Each microscope automatically switches between 110V and 220V electrical supplies (only the Nipow disk motor requires an optional 110V/220V adaptor), fits into two suitcases (Pelican Products, Inc., Torrance, CA, USA), and may be set up and tested within one hour of arrival at museum locations.

Materials and Methods

The work reported here was performed with the 1K2. Four naturally fractured molars, one previously sectioned molar and one canine, all of which have been attributed to *A. africanus*, were used in this preliminary study of enamel microstructural features (Table 1). These specimens derive from what is currently known as Member 4 of the Sterkfontein Formation, dated to about 2.5 my (Vrba, 1995). The specimens were cleaned with acetone to remove any substances or matrix residue; however, manganese accretions, if present, were not removed. The fractured surface of the tooth was placed approximately perpendicular to the optical axis over which was placed a drop of immersion oil and a cover slip. To study cross striation periodicity, a 50x Mituyomo lens was typically used with a 1:1 adapter. Striae/EDJ angles were imaged using both the 20x and 10x lenses with both 0.5 and 1:1 adapters. The K2S-BIO automatically imposes a 2x magnification, effectively doubling the image presented to the CCD. Most images acquired for purposes of recording cross striation periodicity were observed close to the outer enamel surface between the cervical and lateral regions of the crown. Images were Z-montaged in Syncroscopy Auto montage and analyzed with Adobe v 7.1

It is generally accepted that the angles formed between the striae and the EDJ provide useful information on the variation of ameloblast extension rates (Boyde 1964).

To study striae/EDJ angles, the EDJ surface was divided into three equal sections: cuspal, middle and cervical, following Beynon and Wood (1986) and Ramirez Rozzi (2002). The angles were measured as shown in Schwartz *et al.*; (2003: Fig. 2A). In addition, for purposes of comparison to the canine STW 267, the SK 63 canine attributed to *Paranthropus robustus*, which was previously sectioned and described by Dean *et al.*; (1993b), was imaged with a Wild stereo microscope.

Australopithecus africanus specimens examined include: STW 11 (RM³), STW 90 (RM₃), STW 190 (Left maxillary molar fragment), STW 284 (LM²), and STW 37 (LM³). Crown formation time is provided for Stw 284 because it had been previously sectioned along the tips of the mesial cusps providing good control over the faces studied and showed minimal cuspal wear.

Results

There is much interest in obtaining details of hominid enamel microstructure from fractured surfaces, but such surfaces are rarely forgiving and the resolving power has been wanting. However, the PCSOM provides through focus imaging of topographically complex surfaces at relatively high magnifications revealing a plane view of enamel microstructure (e.g. striae of Retzius and cross striations). Further, because the K2S-BIO employs circularly polarized light, some enamel crystallite orientation contrast is provided (Bromage *et al.*; 2005).

CROSS STRIATION PERIODICITY AND STRIAE/EDJ ANGLES

Cross striations were identified as varicosities and constrictions along a prism. Our study recorded 6 cross striations for the *A. africanus* M³ STW 11 (Figure 5) and 6 or 7 for the M² STW 284 (Figure 6) between adjacent striae of Retzius. It was difficult to confidently ascertain the exact number of cross striation in Stw 284 because in the best field we could find that showed both cross striations and Striae, the use immersion oil and limitations on the light power source formed a slightly diffuse image. The anterior dentition represented by the single canine STW 267 was very difficult to image as most of the outer enamel surface is damaged and overlain with matrix. However, using measurements of cross striation lengths and distances between adjacent striae of Retzius, it was possible to calculate a repeat interval of 9. Dean *et al.*; (1993b) observed

the same number of cross striations in their original study of the *Paranthropus* canine SK 63.

We took also the opportunity to measure the angles formed between the striae of Retzius and the EDJ. Table 1 shows the values of the striae/EDJ angles obtained for each of the specimens included in this study and, as expected based on the works of Beynon and Wood (1986) and Ramirez Rozzi (2002), the angles are more acute in *Paranthropus* than in *Australopithecus*. In the canine, the values increase in both genera from the cusp to the cervix as already noted for other taxa (Beynon *et al.*; 1991; Macho and Wood, 1995). However, the change observed in *Paranthropus* is of a lesser magnitude than observed for the *Australopithecus* specimens.

For molars, *A. africanus* striae/EDJ angles may be compared with those of east African *Paranthropus* specimens investigated by Ramirez Rozzi (2002). Table 2 indicates the results of Mann-Whitney *U* test between the means of each section along the EDJ in molars of each genus. The differences are statistically significant in the cervical third, but not significant in the middle or cuspal regions. The enamel extension rate of *A. africanus* ($n = 5$) decreases (i.e. angles increase in value) from the cusp to the cervix more than *Paranthropus*, which shows almost no change in the mean values from the middle section of the crown to the cervix ($n = 12$). These differences are statistically significant in *Australopithecus* ($p < 0.05$).

CROWN FORMATION TIME OF STW 284

Most recent studies of hominoid crown formation use the method of Beynon and Wood (1987), which identifies two arbitrary areas of the crown divided by the point at which the first striae of Retzius reaches the enamel surface. These areas are lateral (or imbricational) and cuspal (or appositional) enamel and here we follow this terminology.

To calculate crown formation time in STW 284, we multiplied the number of lateral striae of the protocone (e.g. Figure 7) by the cross striation periodicity. In addition, cuspal enamel thickness was measured following the path of enamel rods from the point where the first lateral stria appears, to the EDJ (e.g. Figure 8). Because prisms decussate near the EDJ in Stw 284, this measurement was multiplied by the Risnes (1986) correction factor (1.15) which takes into account prism decussation. The result was divided by the average daily secretion rate on cuspal enamel. This value was obtained by measuring many groups of three to five adjacent cross striations identified in

various fields of inner, mid and outer cuspal enamel. The mean cuspal appositional rate of 5.6 microns for this specimen represents the total of inner, middle and outer cuspal values combined. Six or 7 cross striations were identified between striae of Retzius in the upper second molar STW 284. Counts of striae on the paracone gave a total of 82. Taking into consideration the number of cross striations between striae (6 or 7), this gives a range of 495 or 577 days, or 1.34 to 1.57 years, respectively, for the formation of lateral enamel. Cuspal enamel thickness was estimated to be 2.67 mm, which was then multiplied by the Risnes (1986) correction factor. This value was divided by the mean of cuspal daily secretion rates. Using this method, the duration of cuspal enamel was estimated to be 1.5 years. As cusp formation time is the sum of cuspal and lateral enamel, this gives a total of 2.84 (6 cross striations) or 3.07 (7 cross striations) years for the development of the protocone.

As noted before (Ramirez Rozzi, 1993), using counts of striae or perikymata on anterior cusps alone to determine crown formation time can underestimate the total period of formation as posterior cusps complete their formation with some delay in relation to the anterior cusps (e.g. Kraus and Jordan, 1965). The last visible stria on the protocone was followed to its corresponding perikyma and this was followed to the hypocone (e.g. Figure 9). The perikymata cervical to it on this cusp were counted giving a total of 12 perikymata, or an additional 0.2 years of growth. This gives a total of 3.0 (6 cross striations) or 3.3 (7 cross striations) years for the crown development of STW 284.

Discussion

While the improvement over conventional light microscopy in imaging thin sections may not be substantial, the improvement made by the Portable Confocal Microscope for the examination of the surface layers of bulk samples non-destructively is nothing short of revolutionary. Even if images cannot be obtained through a great depth, the convenience factor of not having to produce a thin section as a prerequisite for excellent optical microscopy is a very great advantage in our research.

Two PCSOM microscopes are in service to date. The first (1K2) was described by Bromage *et al.* (2003); it is automated in Z and operates a notebook-based PC monochrome image acquisition system. The work reported here was performed with this system. This microscope is dedicated to specific long-term projects (e.g. dissertations). The other microscope (2K2) is fully automated in X, Y, and Z. With development of the PCSOM the potential for non-destructive mineralized tissue research on rare and unique early hominid remains is great.

An important feature of enamel development is the number of cells involved in matrix secretion and the rate at which these cells become differentiated along the enamel-dentine junction (EDJ). All active cells during amelogenesis periodically stop normal secretory activity, creating features known as striae of Retzius (cf. Boyde, 1990). Their periodicity can be calculated by recording the number of daily cell secretions or cross striations between each stria (cf. Bromage 1991). Originally, Boyde (1964) proposed a method to estimate the rate of cell differentiation based on the angles formed between the brown Striae of Retzius and the EDJ. More acute angles indicate a higher ameloblast extension rate. A later study (Beynon and Wood, 1986) made use of this method in an analysis of isolated teeth attributed to *Paranthropus* and *Homo* to assess differences between these two genera. They found that the angles formed between the EDJ and the striae were more acute in *Paranthropus* than in *Homo*, with means of 23 and 31 degrees respectively. Their measurements were taken on the occlusal third of the crown. Ramirez Rozzi (1993, 1998, 2002) used a larger sample derived from the Omo-Shungura Formation to assess possible temporal changes in the rates of ameloblast differentiation in isolated teeth from a well stratified and dated chronological sequence. Measurements were taken on three sections along the EDJ (cuspal, central –equivalent to our “middle” region of Table 2- and cervical areas). In agreement with Beynon and Wood (1986), Ramirez Rozzi found fast rates of enamel differentiation in the genus *Paranthropus*. Although, he also noted differences between *P. aethiopicus* and *P. boisei*. The only published record on striae/EDJ angles in *A. africanus* is that of Grine and Martin (1988) and, although no measurements of the angles were indicated, they observed that *Paranthropus* showed more acute angles than *A. africanus*. Thus, at present, there is almost no data on the microstructural features of this species.

An important aspect in studies of dental development using microstructure is the cross striation periodicity. Most commonly, this value is assessed from histological ground sections or by scanning electron microscopy, but both methods are intrusive and laborious. Thus only four studies to date have included information regarding cross striation periodicity on hominid fossils; a *P. boisei* premolar (Beynon and Dean, 1987), a *P. boisei* molar (Dean 1987); a *P. robustus* canine (Dean *et al.*; 1993b), and a Neandertal molar (Dean *et al.*; 2001). Here we report a relatively significant sample of cross striation periodicities for a single hominid species.

Values of cross striation periodicity observed in the small sample of teeth attributed to *A. africanus* are highly variable. For the two molars observed the numbers ranged from six to seven. The anterior dentition, represented here by a single canine (STW 267), presented a calculated value of nine cross striations which is the same number observed by Dean *et al.*; (1993b) in the *Paranthropus* canine SK 63. This variation falls within the cross striation periodicity values recorded for modern humans (6-12) (Dean and Reid, 2001) and is similar to chimpanzees (6-8) (Reid *et al.*; 1998b; Smith, 2004).

Results from this preliminary study indicate that there may be some differences in growth mechanisms of enamel tissue between *A. africanus* and *Paranthropus*. In general, enamel extension rates in *A. africanus*, measured as the angles formed between striae of Retzius and the EDJ, decrease as the development of the crown approaches the more cervical aspects of the tooth; that is, the angles have higher values in *A. africanus* than in *Paranthropus* (Table 1). It could be argued that some of these differences are the result of studying naturally-fractured teeth where there is no control of the plane of section. However, the fact that all *A. africanus* molars studied show the same pattern of difference from East African *Paranthropus* molars, suggests that the plane of fracture does not significantly affect the results.

The crown formation time of a single molar of *A. africanus* was estimated to be 3.0 to 3.3 years. The former value is similar to the mean of crown formation time of molars attributed to *P. boisei* and greater than values of *P. aethiopicus* (Ramirez Rozzi, 1993). The crown formation time of STW 284 is less than values on second molar development reported in modern humans derived from histological studies (Dean *et al.*; 1993a; Reid *et al.*; 1998a). This is in spite of the fact that *A. africanus* molars have thicker enamel and greater occlusal area than *H. sapiens*. All of this taken together emphasizes differences already noted between extant and extinct taxa on the one hand, and between different hominid species on the other (Beynon and Wood, 1987; Beynon and Dean, 1988; Bromage and Dean, 1985; Dean *et al.*; 2001).

Conclusions

The Portable Confocal Scanning Optical Microscope was specifically developed to offer superb analytical light microscopy of early hominid skeletal material. Limitations over the handling and transport of rare fossils have motivated this development in order that

specimens may be examined wherever and whenever the microscope must go to the place and the subject.

This study has added new information on the growth processes of enamel identified in the southern African hominid taxa *A. africanus*. Given the results obtained here, it would be important to assess growth processes for the South African taxon *P. robustus*, for which almost no information on molar development is available, to possibly help better establish relationships among early African hominids.

Acknowledgements

Support for this work was generously provided by the L.S.B. Leakey Foundation, the Blanquer and March Foundations (Spain) and the Palaeoanthropology Scientific Trust (PAST, South Africa). For the availability of hominid specimens and assistance, the Department of Palaeontology, Transvaal Museum, Pretoria, South Africa, and the Department of Anatomy, University of the Witwatersrand, Johannesburg, South Africa, are gratefully acknowledged.

References:

- Berger, L., Lacruz, R.S., de Ruiter D.J., 2002. Revised Age Estimates of Australopithecus Bearing Deposits at Sterkfontein, South Africa. *Am. J. Phys. Anthropol.* 119, 192-197.
- Beynon, A.D., Dean M.C., 1987. Crown formation time of a fossil hominid premolar tooth. *Arch. Oral Biol.* 32, 773-780.
- Beynon, A.D., Dean, M.C., 1988. Distinct dental development patterns in early fossil hominids. *Nature* 335, 509-514.
- Beynon, A.D., Dean, M.C., Reid, D.J., 1991. A histological study on the chronology of the developing dentition of gorilla and orang-utan. *Am. J. Phys. Anthropol.* 86, 295-309.
- Beynon, A.D., Wood, B., 1986. Variations in enamel thickness and structure in East African hominids. *Amer Am. J. Phys. Anthropol.* 70: 177-193.
- Beynon, A.D., Wood, B., 1987. Patterns and rates of enamel growth on the molar teeth of early hominids. *Nature* 326, 493-496.
- Boyde, A., 1964. The structure and development of mammalian enamel. Ph.D. Dissertation, University of London.
- Boyde, A., 1990. Developmental interpretations of dental microstructure. In: C. Jean de Rousseau (Ed), *Primate Life History and Evolution*. Wiley-Liss Publ., New York, pp.
- Boyde, A., 1995. Confocal optical microscopy. In: Wootton, R., Springall, D.R., Polak, J.M. (Eds), *Image Analysis in Histology: Conventional and Confocal Microscopy*. Cambridge University Press, Cambridge, UK, pp. 151-196.
- Boyde, A., Petran, M., Hadravsky, M., 1983. Tandem scanning reflected light microscopy of internal features in whole bone and tooth samples. *J. Microsc.* 132, 1-7.
- Bromage, T.G., 1991. Enamel incremental periodicity in the pig-tailed macaque: a polychrome fluorescent labelling study of dental hard tissues. *Am. J. Phys. Anthropol.* 86, 205-214.
- Bromage, T.G., Dean, M.C., 1985. Re-evaluation of the age at death of immature fossil Hominids. *Nature* 317, 525-527.
- Bromage, T.G. Perez-Ochoa, A., Boyde, A., 2003. The Portable confocal microscope: Scanning optical microscopy anywhere. In: Méndez-Vilas, A. (Ed), *Science, Technology and Education of Microscopy: An Overview*. Formatex, Badajoz, Spain, pp. 742-752.
- Bromage, T.G. Perez-Ochoa, A., Boyde, A., 2005. Portable confocal microscope reveals fossil hominid microstructure. *Microsc. Anal.* May.
- Dean, M.C. 1987. Growth layers and incremental markings in hard tissues: are view of the literature and some preliminary observations about enamel structure in *Paranthropus boisei*. *J. Hum. Evol.* 16, 157-172.
- Dean, M.C., Beynon, A.D., Reid, D.J., Whittaker, D.K., 1993a. A longitudinal study of tooth growth in a single individual based on long and short period markings in dentine and enamel. *Int. J. Osteoarch.* 3, 249-264.
- Dean, M.C., Beynon, A.D., Thackeray, J.F., Macho, G.A., 1993b. Histological reconstruction of dental development and age at death of a juvenile *Paranthropus robustus* specimen, SK 63, from Swartkrans, South Africa. *Am. J. Phys. Anthropol.* 91, 401-419.
- Dean, M.C., Leakey, M., Reid, D., Schrenk, F., Schwartz, G., Stringer, C., Walker, A., 2001. Growth processes in teeth distinguish modern humans from *Homo erectus* and earlier hominins. *Nature* 44, 628-631.

- Dean, M.C., Reid, D.J., 2001. Perikymata and distribution on Hominid anterior teeth. *Am. J. Phys. Anthropol.* 116, 209-215.
- Delson, E. 1984. Cercopithecoid biochronology of the African Plio-Pleistocene: correlation among eastern and southern hominid-bearing localities. *Cour Forsch Inst Senckenberg* 69, 199-218.
- Delson, E., 1988. Chronology of South African australopith site units. In: Grine, F.E. (Ed), *The Evolutionary History of the "Robust" Australopithecines*. Aldine de Gruyter, New York, pp. 317-324.
- Grine, F.E., Martin, L.B., 1988. Enamel thickness and development in *Australopithecus* and *Paranthropus*. In: Grine, F.E. (Ed), *The Evolutionary History of the "Robust" Australopithecines*. Aldine de Gruyter, New York, pp. 3-42.
- Kino, G.S., 1995. Intermediate optics in Nipkow disk microscopes. In: Pawley, J.B. (Ed), *Handbook of Biological Confocal Microscopy*. Plenum Press, New York, pp. 155-165.
- Kraus, B.S., Jordan, R.E., 1965. *The human dentition before birth*. Lea & Febiger Publ., Philadelphia.
- Macho, G.A., Wood, B.A., 1995. The role of time and timing in hominid dental evolution. *Evol. Anthropol.* 4, 17-31.
- Nipkow, P., 1884. Elektrisches Teleskop. Patentschrift 30105 (Kaiserliches Patentamt, Berlin), patented 06.01.1884.
- Petran, M., Hadravsky, M., 1966. Method and arrangement for improving the resolving power and contrast. United States Patent No. 3,517,980, priority 05.12.1966, patented 30.06.1970 US.
- Ramirez Rozzi, F., 1993. Tooth development in East African *Paranthropus*. *J. Hum. Evol.* 24, 429-454.
- Ramirez Rozzi, F., 1998. Can enamel microstructure be used to establish the presence of different species of Plio-Pleistocene hominids from Omo, Ethiopia? *J. Hum. Evol.* 35, 543-576.
- Ramirez Rozzi, F., 2002. Enamel microstructure in hominids: New characteristics for a new paradigm. In: Minugh-Purvis, N, McNamara, K.J. (Eds), *Human Evolution Through Developmental Change*. Johns Hopkins University Press, Baltimore, pp. 319-348.
- Reid, D.J., Beynon, A.D., Ramirez Rozzi, F.V., 1998a. histological reconstruction of dental development in four individuals from a medieval site in Picardie, France. *J. Hum. Evol.* 35, 463-478.
- Reid, D.J., Schwartz, G.T., Dean, M.C., Chandrasekera, M.S., 1998b. A histological reconstruction of dental development in the common chimpanzee. *J. Hum. Evol.* 35, 427: 448.
- Risnes, S., 1986. Enamel apposition rate and the prism periodicity in human teeth. *Scand. J. Dent. Res.* 94, 394-404.
- Schwartz, G.T., Liu, W. & Zheng, L. (2003). Preliminary investigation of dental microstructure in the Yuanmou hominoid (*Lufengpithecus hudiensis*), Yunnan Province, China. *J. Hum. Evol.* 44, 189-202.
- Smith, T.M., 2004. Incremental development of primate dental enamel. Ph.D. Dissertation, State University of New York, Stony Brook.
- Tobias, P.V., 1980. *Australopithecus afarensis* and *A. africanus*: critique and an alternative hypothesis. *Palaeont. afr.* 23, 1-17.
- Vrba, E.S., 1995. The fossil record of African antelopes (Mammalia, Bovidae) in relation to human evolution and paleoclimate. In: Vrba, E.S. (Ed), *Paleoclimate*

And Evolution, With Emphasis On Human Origins. Yale University Press,
New Haven, pp. 385-424.

White, T.D., Johanson, D.C., Kimbel, W.H., 1981. *Australopithecus africanus*: its phyletic
position reconsidered. South Af. J. Sci. 77, 445-471.

Figure Legends

- Figure 1. Diagram of the 1K2 PCSOM (see text for details).
- Figure 2. Diagram of the 2K2 PCSOM (see text for details).
- Figure 3. Fractured enamel surface of a *Paranthropus robustus* molar (SKW 4769; Transvaal Museum). A three-dimensional view of topographic relief in this surface reflection image may be obtained by mental reconstruction of left and right images into one stereoscopic image. FW = 100 μm each frame.
- Figure 4. Same field of view as Figure 3, imaging deep to the surface and revealing incremental enamel microstructure. FW = 100 μm .
- Figure 5. Cross striations between striae of Retzius on outer enamel of the *Australopithecus africanus* molar (STW 11; University of the Witwatersrand). Six cross striations were counted between adjacent striae of Retzius (white arrows) in this specimen. FW = 150 μm .
- Figure 6. Cross striations on cuspal enamel of the *Australopithecus africanus* molar (STW 284; University of the Witwatersrand). Prisms course from upper left to lower right and several marked Retzius lines can be seen coursing from lower left to upper right. FW = 190 μm .
- Figure 7. Striae of Retzius can be seen reaching the outer enamel surface of the *Australopithecus africanus* molar (STW 284; University of the Witwatersrand). FW = 130 μm .
- Figure 8. Cuspal enamel of *Australopithecus africanus* molar (STW 284; University of the Witwatersrand). Prisms can be identified running almost vertically towards the outer enamel surface (top). Cross striations are seen along each prism as dark horizontal lines. FW = 1.3 mm. The boundary between lateral and cuspal enamel is located slightly more cervically and could not be imaged here.
- Figure 9. Perikymata on the cervical enamel of *Australopithecus africanus* (Stw 284). Tomes process pits may be observed as specs between perikymata. FW = 180 μm .

Tables

Table 1. Striae-EDJ angle values for each specimen studied at each division along the EDJ. The numbers in brackets indicate the number of angles measured for each section.

Specimen number	Tooth	Area	Mean (n)
SK 63	UC	Cuspal	14.5 (4)
		Middle	31.8 (9)
		Cervical	34.6 (8)
STW 279	UC	Cuspal	?
		Middle	34.2 (4)
		Cervical	41.4 (5)
STW 284	UM2	Cuspal	20.0 (2)
		Middle	31.3 (6)
		Cervical	40.6 (5)
STW 190	frag	Cuspal	14.6 (3)
		Middle	28.0 (5)
		Cervical	39.3 (4)
STW 90	Lm3	Cuspal	21.0 (2)
		Middle	30.7 (7)
		Cervical	34.7 (7)
STW 11	UM3	Cuspal	16.5 (2)
		Middle	28.5(7)
		Cervical	51.4 (7)
STW 37	UM3	Cuspal	18.0 (2)
		Middle	35.0 (5)
		Cervical	38.0 (4)

Table 2. Results of the Man-Whitney *U* test between the means of *Paranthropus* and *A. africanus* for the striae-EDJ angle values at each division along the EDJ. The values shown for *E.A. Paranthropus* were taken from Ramirez Rozzi (2002) and include, on the lower dentition, six M3, a possible M2 or M3, and two M1 or M2. The upper dentition consists of one M2, one M3, and a possible M2 or M3 (Ramirez Rozzi 2002: Table 15.2)

	Sample	Mean	SD	<i>p</i> value
Cuspal				
	EA <i>Paranthropus</i>	12	13.2	5.2
	<i>A. africanus</i>	5	18.2	2.6
				N.S.
Middle				
	EA <i>Paranthropus</i>	12	26.7	6.9
	<i>A. africanus</i>	5	33.9	4.5
				N.S.
Cervical				
	EA <i>Paranthropus</i>	12	26.0	6.5
	<i>A. africanus</i>	5	42.0	6.0
				<i>p</i> < 0.05

Figure 1

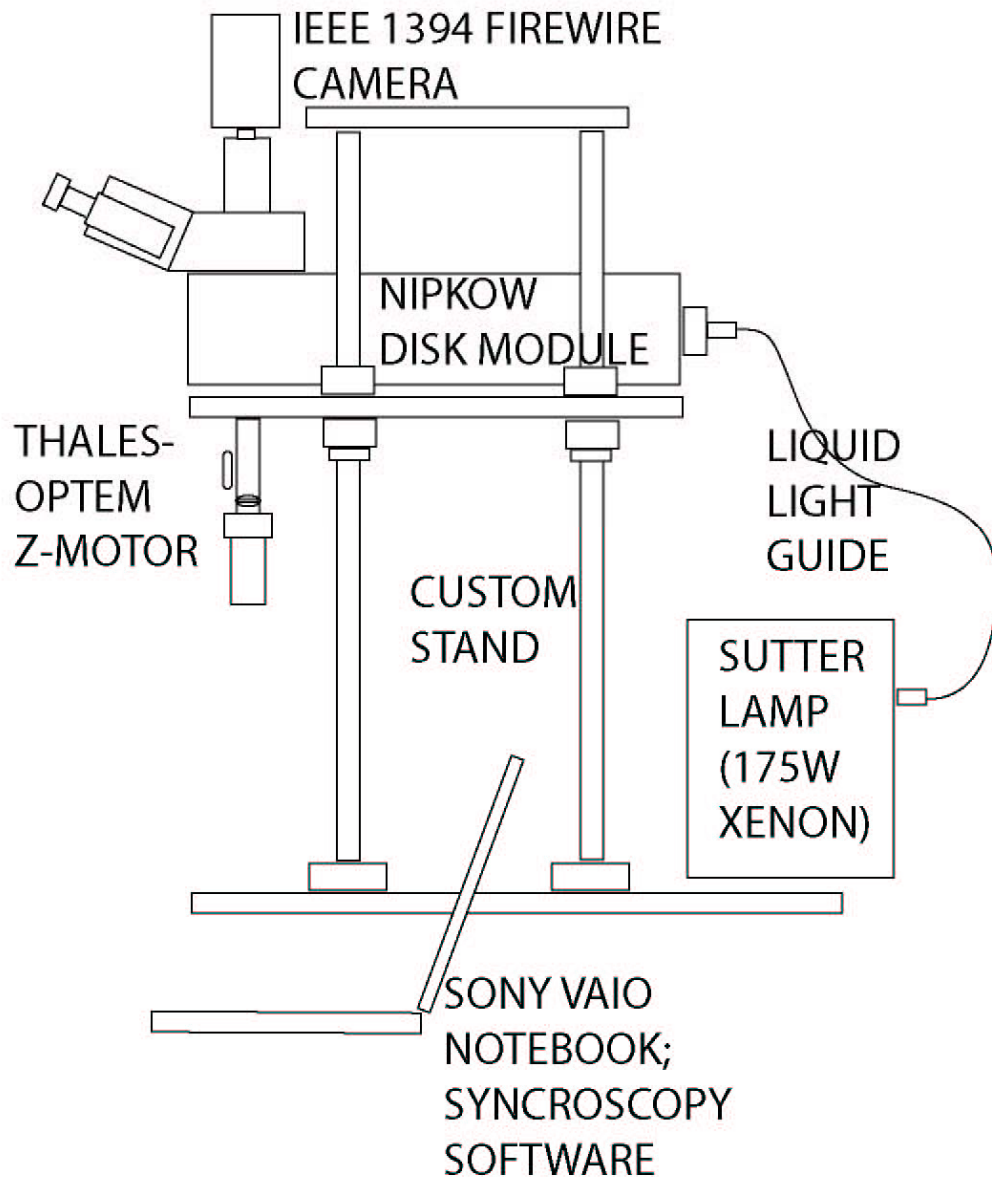


Figure 2

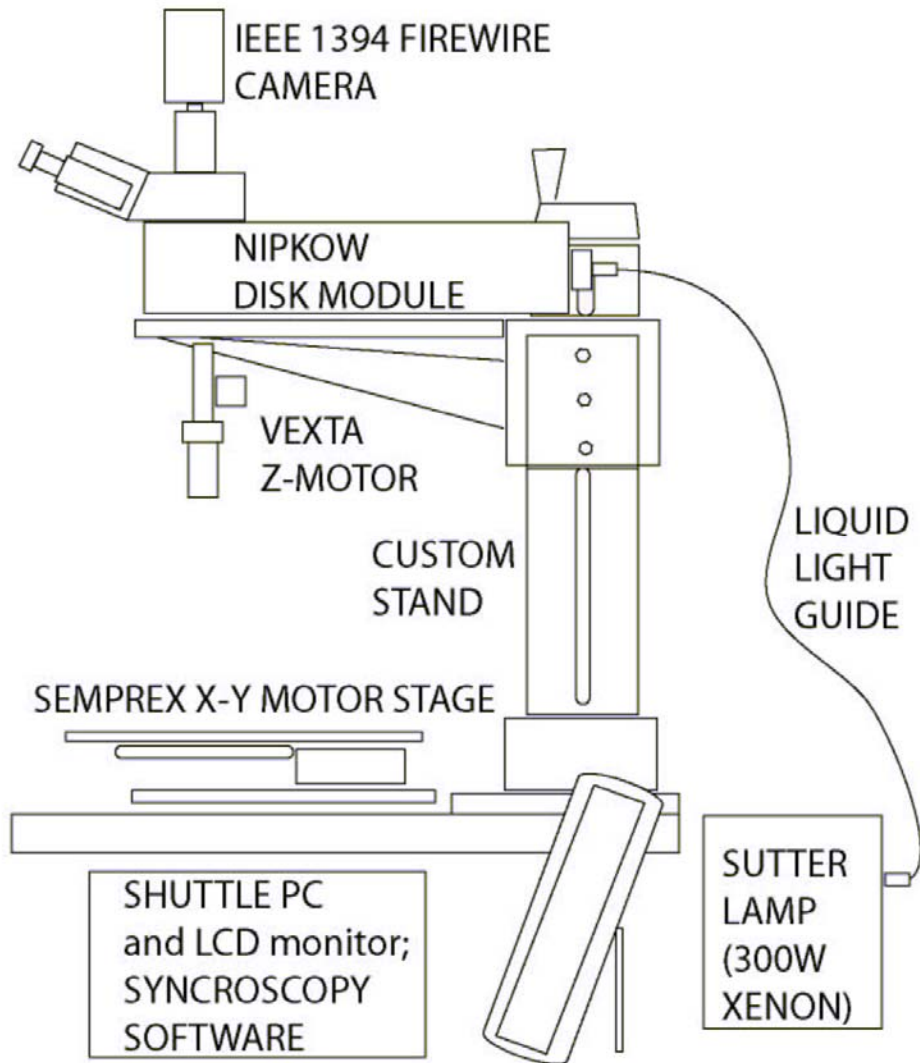


Figure 3

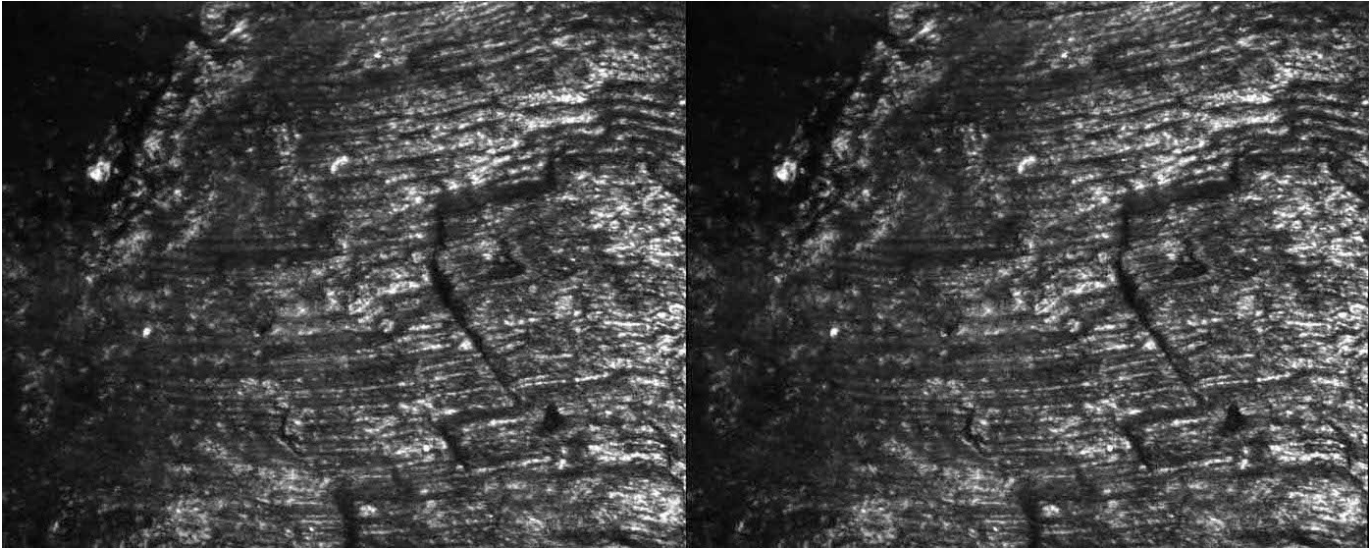


Figure 4



Figure 5

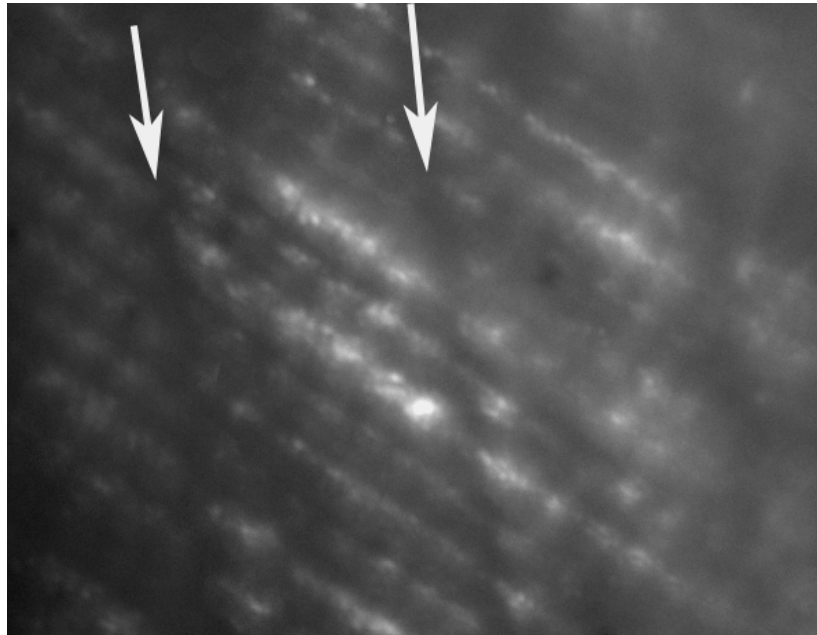


Figure 6

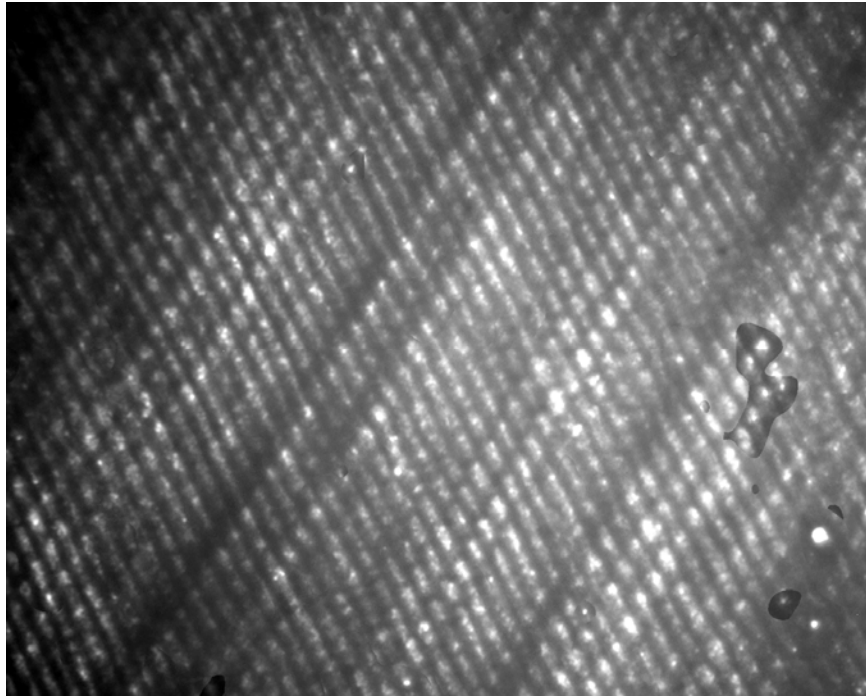


Figure 7

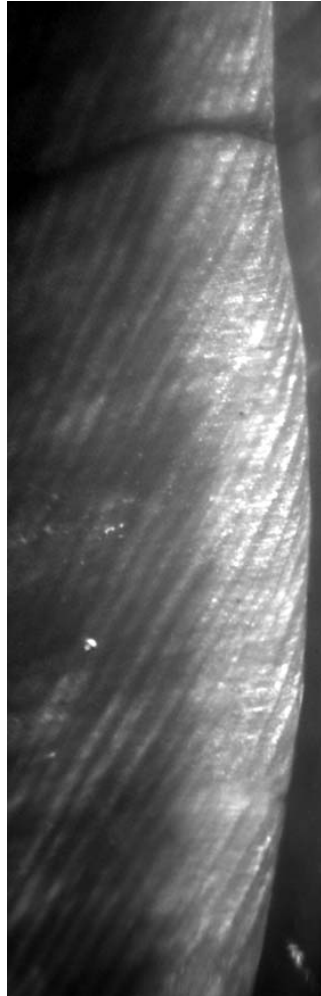


Figure 8

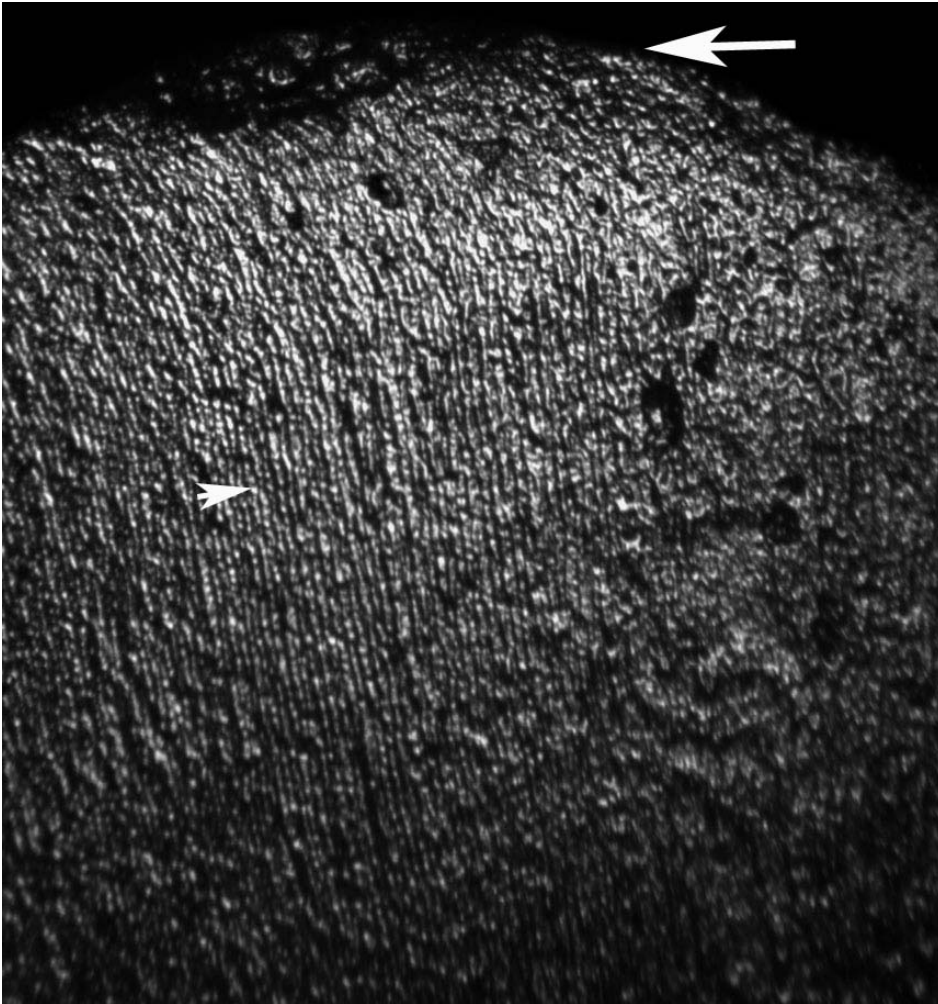


Figure 9

